STM JOURNALS

Journal of
Polymer & Composites

ISSN: 2321-2810 (Online)
ISSN: 2321-8525 (Print)
Volume 13, Special Issue 1, 2025
DOI (Journal): 10.37591/JoPC

https://journals.stmjournals.com/jopc

Research JoPC

Synthesis of Magnetically Recoverable Nickel (II) Complex-Functionalized Fe_3O_4@ISNA (ISNA= Isonicotinic Acid) Nanomaterials: Catalytic Studies on Nitrophenol Reduction and TD- DFT Studies

Rimpa Mondal[1], Rinku Ghanta[2], Madhulata Shukla[3], Tanmay Chattopadhyay[4,*]

Abstract

In this study, we aimed to develop a novel, environmentally sustainable, and magnetically separable heterogeneous nanocatalyst, denoted as Fe_3O_4@ISNA@NiL (where L represents the ligand). The synthesis involved a two-step process, first, isonicotinic acid was chemically grafted onto the surface of iron oxide nanoparticles (Fe_3O_4) to introduce functional groups capable of further chemical modification. Subsequently, a nickel(II) Schiff base monomeric complex was anchored onto the modified surface, resulting in a nanocatalyst with enhanced catalytic properties and magnetic separability, facilitating its recovery and reuse in various catalytic applications.The nanocatalyst was thoroughly characterized using various physicochemical techniques, including Fourier Transform Infrared Spectroscopy (FT-IR), Scanning Electron Microscopy (SEM), Transmission Electron Microscopy (TEM), and Powder X-ray Diffraction (PXRD). These analyses confirmed the successful surface modification of the magnetic Fe_3O_4 core. The DFT calculations of the spectral data of the NiL complex had also been done. We investigated the reduction capabilities of Fe_3O_4@ISNA@NiL using p-nitrophenol as a model substrate, optimizing the reaction conditions via UV-Vis spectroscopy. Under optimal reaction conditions, nearly complete reduction of p-nitrophenol (PNP) to the corresponding product p-aminophenol (PAP) was achieved within 10minutes, with a rate constant of $0.09min^{-1}$. Moreover, the nanocomposite exhibited high stability and reusability, retaining its catalytic efficiencyforup-to5cycleswhen manipulated with an external magnetic field.

***Author for Correspondence**
Tanmay Chattopadhyay
Email: tanmayc2003@gmail.com

[1]Research Scholar, Department of Chemistry, Diamond Harbour Women's University, West Bengal, India
[2]Research Scholar, Department of Chemistry, Diamond Harbour Women's University, West Bengal, India
[3]Assistant Professor, Department of Chemistry, G.B. College, Veer Kunwar Singh University, Bihar, India
[4]Assistant Professor, Department of Chemistry, Diamond Harbour Women's University, West Bengal, India

Received Date: August 05, 2024
Accepted Date: September 24, 2024
Published Date: November 18, 2024

Citation: Rimpa Mondal, Rinku Ghanta, Madhulata Shukla, Tanmay Chattopadhyay. Synthesis of Magnetically Recoverable Nickel (II) Complex-Functionalized Fe_3O_4@ISNA (ISNA= Isonicotinic acid) Nanomaterials: Catalytic Studies on Nitrophenol Reduction and TD- DFT Studies. Journal of Polymer & Composites. 2024; 13(Special Issue 1): S88–S96p.

Keywords: Heterogeneous catalyst, magnetically separable Nanocomposite, Nitrophenol reduction, Reusable, TD-DFT studies.

INTRODUCTION

In recent time nitroaromatic compounds are generally used in industrial processes such as for the manufacturing of dyes, pigments, pesticides, pharmaceuticals, wood preservatives and rubber chemicals [1]. Due to continuous increase in industrialization, nitroaromatic compounds becomes them a in source of water pollutants leading to significant health risks due to their high toxicity and carcinogenicity [2]. Synthesis of aminoarenes from the reduction of corresponding nitroarenes is more important because of their widespread use to produce numerous analgesic and

antipyretic drugs [3,4]. According to literature survey there are several approaches for the reduction of nitrophenols to aminophenols such as iron-acid reduction [5], electrolytic reduction [6], catalytic hydrogenation [7] etc. Among these, homogeneous catalysts provide benefits like high selectivity, turnover number, and yield, along with excellent catalytic performance and surface area. However, they face issues such as instability at high temperatures and challenges with regeneration and separation from the reaction medium [8-10]. Novel metal catalysts are less effective than transition metal-based catalyst because of their low earth-abundance and high cost and its agglomeration tendency limits its catalytic activity [11]. To overcome these issues, designing and developing a suitable surface coating heterogeneous nanocatalyst by immobilizing transition-metal complexes on solid supports can produce robust, easily handled catalysts with an improve the catalytic efficiency and potentially enhanced selectivities which provides better catalytic recoverability and sustainability [12-14]. In this field, Nanocatalysts becomes an attractive concern among modern researchers because of their unique properties like large surface to volume ratio, high surface energy, easily accessible active site etc [15]. Magnetic nanomaterial based heterogeneous catalyst gain much more attention over nanomaterial based heterogeneous catalyst because of their easy separation from the reaction mixture by an external magnetic field rather than filtration, centrifugation which leads to more time consumption and wastage of catalyst [16]. Immobilization techniques are crucial for binding dopant molecules firmly to the metallic core, making them accessible to external reagents and substrates [17]. Magnetic nanomaterials, especially iron oxide-based nanoparticles, has been choose as a promising candidate as a catalyst-supports because of its high stability, low toxicity, high superparamagnetic nature, cost effectiveness and various application in pharmaceuticals and industries [18]. In the present study, we have synthesized a heterogeneous catalyst, Fe_3O_4@ISNA@NiL consists of a magnetic core, and Fe_3O_4 which have been simultaneously fabricated with isonicotinic acid and Ni (II)-Schiff base complex to achieve the cost-effective hydrogenation of nitrophenols to aminophenols by using $NaBH_4$ as a reducing agent. Isonicotinic acid was selected as a grafting agent due to its effective binding to the iron oxide surface, stabilizing the system. This compound, used here as an iron oxide capping agent, has diverse applications including antibacterial drugs, tuberculosis and psoriasis treatments, arthritis management, plant growth regulation, corrosion control, and pesticide preparation [19]. Our synthesized catalyst has been characterized by employing different physical techniques like FT-IR, PXRD, SEM, TEM etc. Fe_3O_4@ISNA@NiL can easily reduce nitroaromatics to aminoarenes in presence of $NaBH_4$. In order to comprehensively grasp the structural and spectral characteristics of the NiL complexes, Density Functional Theory (DFT) calculations was conducted using the Gaussian 16 program [20] due to its inherent precision. The calculations were executed employing the DFT method with the LanL2DZ basis set at the B3LYP level [21], providing vital insights into the structure and spectral properties in the gaseous state. In addition, Time-Dependent DFT (TD-DFT) calculations were carried out at the same level and using the same basis set.

EXPERIMENTAL SECTION

Materials and Methods

All chemicals and reagents used in this study were of analytical grade, procured from Sigma-Aldrich, and utilized without additional purification. Double-distilled water and other solvents used in the experimental processes were thoroughly purified and dried according to established commercial methods. The UV-visible changes of *p*- nitrophenol were recorded at room temperature using a UV-3101PC spectrophotometer (Shimadzu). FT-IR spectra were acquired on a PerkinElmer RXI FT-IR spectrophotometer, with samples prepared as KBr pellets. High-resolution images of Fe_3O_4@ISNA and Fe_3O_4@ISNA@NiL were obtained by SEM and TEM from Nanoscience and Nanotechnology (CRNN), Kolkata. PXRD patterns were collected using a Bruker D8 AVANCE instrument. The magnetization curves were determined using a Vibrating Sample Magnetometer (EV-9, Microsense,ADE).

Procedure for the Synthesis of Heterogeneous Catalyst (Fe_3O_4@ISNA@NiL)

NiL complex [22], Fe_3O_4nanoparticles (NPs) [23] and Fe_3O_4@ISNA [24] were prepared as we described previously in our earlier study. Then, 50 mg of the NiLcomplex was dissolved in water in a

round bottom flask, add 50 mg of Fe_3O_4@ISNA onto it with continuous stirring up to 24 hours. Subsequently, the dark brown precipitate was collected by filtration followed by rigorous cleansing with a 1:1 methanol-water and dried under vacuum Figure 1.

FT-IR(KBr): $\bar{\upsilon}$(C=O of ISNA) 1411 cm^{-1}, $\bar{\upsilon}$ (C=N of pyridine ring)1557cm^{-1}, (skeletal vibrational frequency): 1485 cm^{-1}, $\bar{\upsilon}$(Fe_3O_4) 670 cm^{-1}, 527cm^{-1} (Figure 2A). PXRD: 2θ = 10.42°, 28.84°, 35.39°, 45.75°, 59.14°, and 62.81° (Figure 2B).

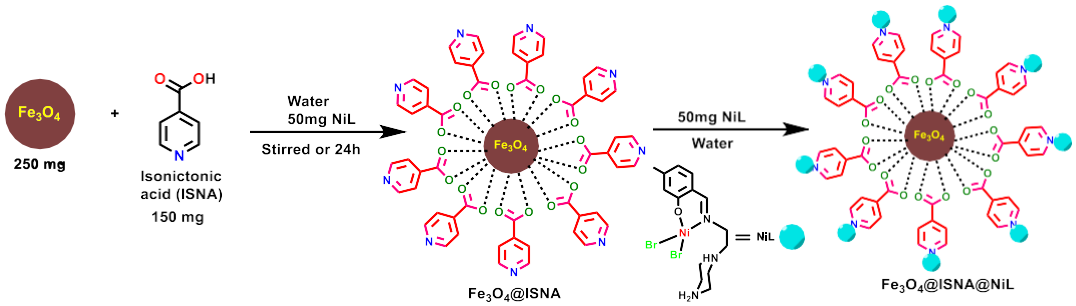

Figure 1. Schematic Representation for the Preparation of Fe_3O_4@ISNA@NiL.

Procedure for the Reduction of Nitrophenol Catalyzed by the Fe_3O_4@ISNA@NiL

In a typical procedure 1 mmol of nitroarenes was dissolved in 15 mL of water. Subsequently, 0.2 mmol of an aqueous solution of $NaBH_4$was added gradually to the mixture. The reaction mixture was stirred continuously for 10 minutes. After this period, 65 mg (6.10 Ni mol%) of the heterogeneous catalyst Fe_3O_4@ISNA@NiLwas added. The reaction was then allowed to proceed for an additional 10 minutes at room temperature. The mixture was subsequently evaporated to dryness.

RESULT AND DISCUSSION

DFT Calculations

The frequency calculations for the optimized NiL complex structure was performed using the same level of theory and the same basis set mentioned previously. The experimental IR spectra of NiL complex compared with the DFT calculated peaks, as shown in Figure 2. Peak at 668 cm^{-1}, 1099 cm^{-1}, 1265 cm^{-1}, 1653 cm^{-1} corresponds to O-H bond twisting in H_2O, CH_2 wagging coupled with C-C stretching, benzene ring breathing, C=C stretching in benzene ring respectively. Additionally, the peaks at 2874 cm^{-1}, 2938 cm^{-1}, 3265 cm^{-1} and 3409 cm^{-1} represent H-C-H asymmetric stretching in CH_2 group, H-C-H symmetric stretching in CH_2 group, H-N-H asymmetric stretching and H-O-H asymmetric stretching in H_2O molecule respectively. A scaling factor of 0.978 was applied to the DFT data for frequencies above 2900 cm^{-1} to achieve better agreement with the experimental values. Discrepancies in these complexes can be attributed to the fact that calculations were carried out in the gaseous phase, whereas the experimental data was collected for the solid state. Abroad peak above 3000 cm^{-1} corresponds to water present in the sample. The TD-DFT calculation was performed at the same level of calculations using the same basis set, and the calculated data were compared with the experimental UV-visible spectrum of NiL complex. TD-DFT calculated transitions marked by vertical lines in Figure 1B. Different TD-DFT absorbance peaks are observed at variable wavelengths. The absorption peak at 375 nm corresponds to HOMO-5 to LUMO which corresponds to then on bonding or bital of Bromine/watertoσ*orbital C-N/C-C on cyclohexane ring. The transition at 362nm corresponds to HOMO-4 localized on nonbonding orbital of Bromine/ dx^2-y^2orbital of Ni to LUMO+1 electronic transition localized on π* of benzene molecule. The peak at 310 nm represents HOMO-6 located on π electron of the benzene ring to LUMO+1 localized on π* of benzene molecule. Different frontier molecular orbital pictures of NiL complex have been shown in Figure 1C corresponding to different transitions.

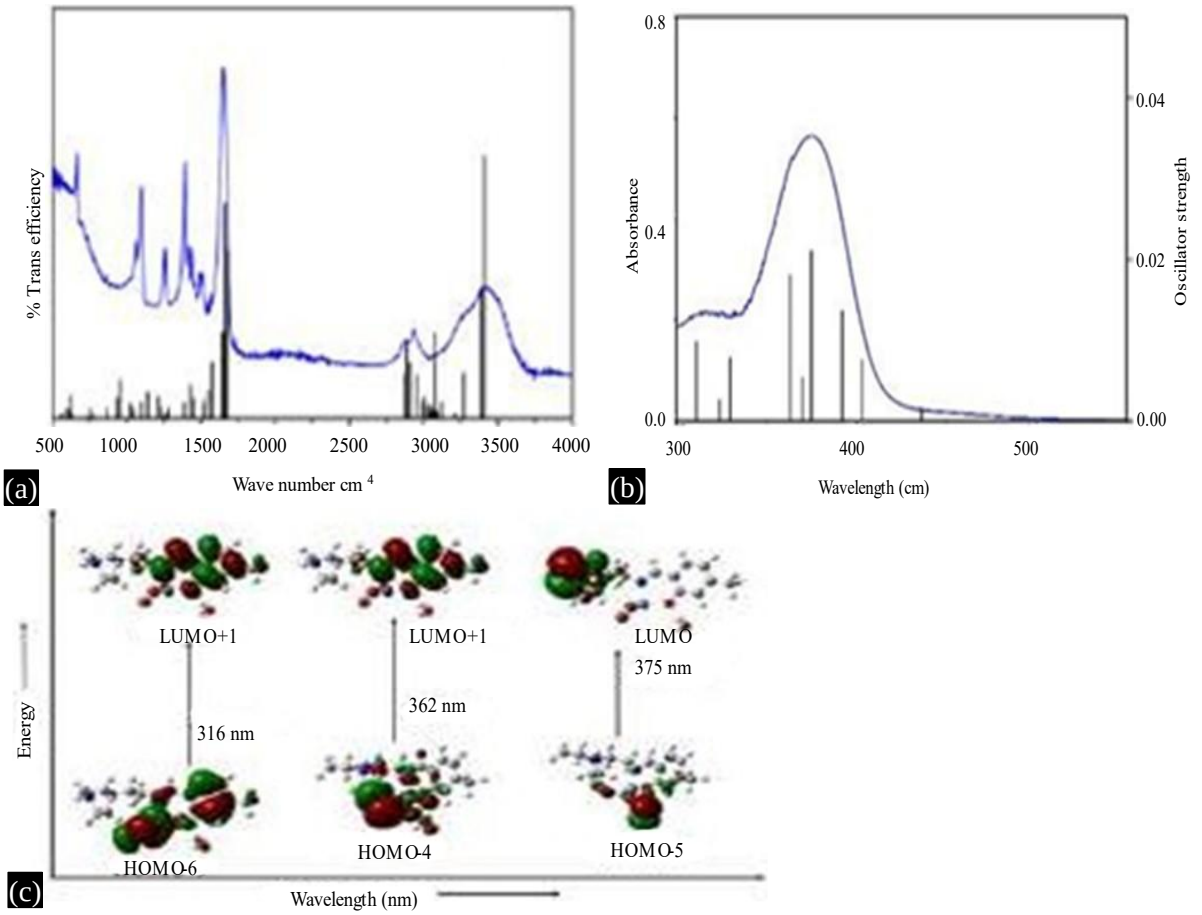

Figure 2. (a) Correlation Between Experimental and DFT Calculated IR Frequencies for NiL Complex, (b) Experimental UV-visible Spectrum of NiL Complex Compared With TD-DFT Calculated Transitions Marked by Vertical Lines, (c) Frontier Molecular Orbital Picture of Different HOMOs and LUMOs Orbitals.

Characterization of Heterogeneous Catalyst Fe_3O_4@ISNA@NiL

FT-IR and PXRD Studies

The FT-IR spectrum of Fe_3O_4@ISNA@NiL is depicted in Figure 3A. The strong absorption band at 527 cm^{-1} confirmed the presence of Fe–O bond. This result characterized the formation of magnetite nanoparticles [25]. The spectral band in the region of 1411cm^{-1} is attributed due to the C=O stretching of the carboxylic acid group in isonicotinic acid. This adsorption peak is significantly lower compared to pure isonicotinic acid, indicating the symmetrical binding of the C=O group to the surface of iron oxide. Additionally, the absorption band at 1557 cm^{-1} can be assigned to the vibrations of the pyridine ring carbons [26]. The distinct absorption band appears at 1650 cm^{-1}, corresponding to the C=N stretching vibration of the imine group within the ligand backbone [27] and the band at 1485 cm^{-1} is attributed to the skeletal vibrations of the benzene ring in the Schiff base complex [28]. The XRD patterns for Fe_3O_4, Fe_3O_4@ISNA are same as reported previously [24]. The XRD patterns of Fe_3O_4@ISNA@NiL are presented in Figure 3B, displays characteristic diffraction peaks at 2θ angles of 10.42°, 28.84°, 35.39°, 45.75°, 59.14°, and 62.81°, corresponding to the (111), (220), (311), (400), (511), and (440) planes, respectively. These peaks are consistent with the standard cubic spinel structure of Fe_3O_4 [29] indicating that the surface modifications with isonicotinic acid and the NiL complex does not significantly alter the crystalline structure of the Fe_3O_4 core. The sharp peaks indicate that the produced material has a polycrystalline structure [30].

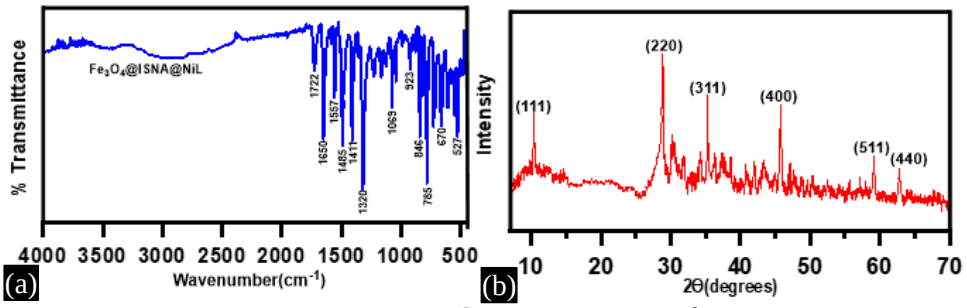

Figure 3. (A)FT-IR Spectrum Data and (B) PXRD Data of Fe_3O_4@ISNA@NiL.

SEM and TEM Studies

Scanning electron microscopy (SEM) analysis was conducted to examine the morphology of the sample [31]. SEM analysis revealed that (Figure 4A), the modified Fe_3O_4@ISNA@NiL exhibits distinct, sharp-edged, plate-like structures on its surface, with agglomeration of isonicotinic acid suggesting the successful incorporation of the NiL complex the surface of Fe_3O_4. The TEM image of Fe_3O_4@ISNA@NiL (Figure 4B) displays numerous small, dark spots on the rod shaped surface, indicating the presence of loosely aggregated NiL metal complex particles which supports the uniformly distribution of NiL complex onto the surface of Fe_3O_4@ISNA.

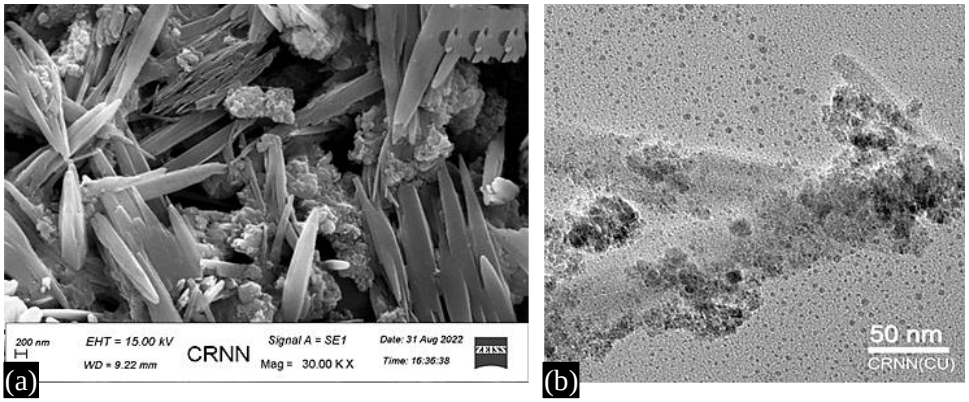

Figure 4. (A) SEM and (B) TEM Image of Fe_3O_4@ISNA@NiL.

Magnetic Study

Magnetic properties of Fe_3O_4 and Fe_3O_4@ISNA@NiL were assessed at ambient conditions using a vibrating sample magnetometer, as illustrated in Figure 5. The saturation magnetization (M_S) of the Fe_3O_4nanoparticles was found at 57.81 emu/g. Upon incorporating the isonicotinic acid and [NiL] complex, a reduction in the magnetization value was found from 57.81 emu/g to 26.34 emu/g due to the shielding effect of the organic counterpart, i.e., diamagnetic part on the surface of iron oxide [32]. Despite this progressive reduction in magnetic strength due to surface modification and complex formation, the magnetization remains sufficiently high for effective magnetic separation from the reaction medium by the application of an external magnetic field.

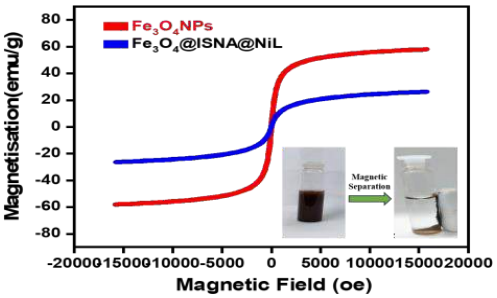

Figure 5. Magnetic Hysteresis Loop of Fe_3O_4 NPs (Red) and Fe_3O_4@ISNA@NiL (Blue).

Catalytic Reduction

To evaluate the catalytic activity of the Fe_3O_4@ISNA@NiL catalyst, the reduction of 4-NP using sodium borohydride ($NaBH_4$) was performed under varying conditions. Reaction parameters were optimized by adjusting catalyst amounts while keeping substrate concentration constant [Table 1]. The catalytic reduction was performed by adding 1mL (0.2mmol) $NaBH_4$ solution in1.5 mL of double-distilled water was mixed with 0.1 mL of a 1 mmol 4-NP solution in a quartz cuvette. Subsequently, 0.05 mL of the catalyst (65 mg, 6.10 mol % of Ni) was added to this mixture [Figure 6]. Reaction progress was monitored at regular intervals via UV-vis spectroscopy to obtain real-time kinetic data. Under these optimized conditions, the catalytic activity was further evaluated by testing a range of nitroaromatic substrates to explore the broader applicability of the catalyst [Table 1].

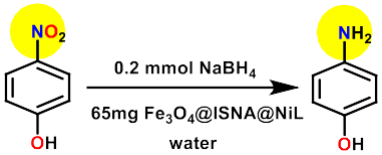

Figure 6. Model Reaction Selected for Optimization of Reaction Conditions for the reduction of p-Nitrophenol by Heterogeneous Catalyst Fe_3O_4@ISNA@NiL.

Table 1. Optimization of the Reaction Conditions for the Reduction of *p*-nitrophenol (1.5 mmol) by Fe_3O_4@ISNA@NiL.

Entry	Fe_3O_4@ISNA@NiL (mg)	Ni mol %	Amount Of $NaBH_4$(mmol)	Yield[a](%)	TON	TOF (h^{-1})
1.	0	--	0.20	≤ 2	--	--
2.	20	1.96	0.20	35	17.50	109.37
3.	35	3.38	0.20	45	12.86	80.37
4.	50	4.76	0.20	62	12.40	77.50
5.	65	6.10	0.20	90	13.84	86.50
6.	100	9.09	0.20	68	6.80	42.50

Bold Signifies Optimum Reaction Conditions.

Catalytic Performance of Fe_3O_4@ISNA@NiL Monitoring via UV-Vis Spectroscopy and Its Kinetic Study

The catalytic performance of Fe_3O_4@ISNA@NiL was assessed by reducing 4-nitrophenol (4-NP) to 4-aminophenol (4-AP) in presence of sodium borohydride ($NaBH_4$). This transformation was monitored using UV-visible spectroscopy, as illustrated in Figure 7A. Initially, the UV-Vis spectrum of an aqueous 4-NP solution exhibited an absorption peak at 325 nm. Following the addition of $NaBH_4$, the solution turned an intense yellow coloration generating a new absorption peak at 405 nm indicating the formation of the p-nitrophenolate ion under alkaline conditions. Upon introducing the Fe_3O_4@ISNA@NiL catalyst into the mixture, the solution gradually transitioned from yellow to colorless within 10 minutes. This was accompanied by an increase in the absorption peak at 325 nm and a decrease in the peak at 425 nm, indicating the formation of 4-aminophenol (4-AP). Kinetic analysis of the reaction was conducted using the first-order

rate equation:

$$\ln [A_t] = -Kt + \ln[A]_0 \; or, ln\frac{[A_t]}{[A]_0} = -Kt$$

Where $[A]_0$ and $[A]_t$ represents the initial concentration and concentration at a time t of the substrate, and K is the rate constant value. A plot of ln (A_t/A_0) *vs* t (Figure 7B) yields a linear relationship with a slope equal to -K, from this plot we determine the rate constant K to be 0.09 min^{-1}.

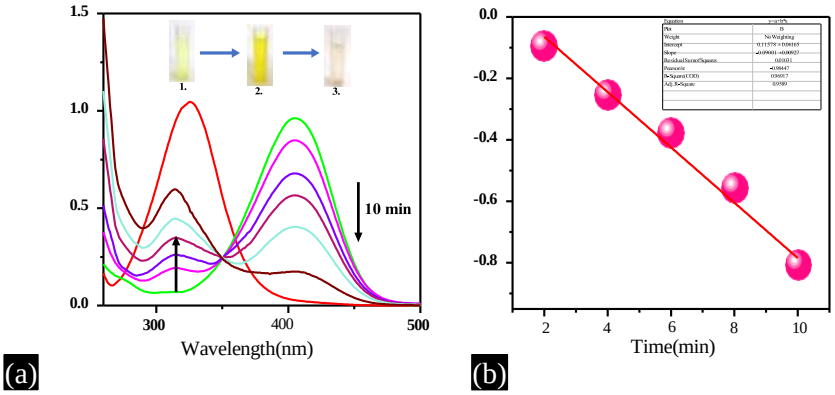

Figure 7. (A) Wavelength Scan; Inset: Digital Color Change from PNP (1) to PAP (3) via the Formation of p-nitrophenolate Ion (2) and (B) Plot of log [A_t/A_0] vs Time (min) for the Reduction of Nitrophenol by $NaBH_4$ Catalyzed by Fe_3O_4@ISNA@NiL.

Reusability

The reusability of the heterogeneous catalyst, a key factor for catalytic applications, was thoroughly examined. After each reaction the catalyst was efficiently separated from the reaction medium using an external magnet. Following each catalytic cycle, the Fe_3O_4@ISNA@NiL catalyst was isolated, washed with water to remove residual reactants, and reintroduced into a fresh 4-nitrophenol (4-NP) solution. Remarkably, the catalyst maintained high conversion rates of 4-NP across five consecutive cycles [Figure 8C], demonstrating its strong reusability and stability under the given reaction conditions. The SEM [Figure 8A] and TEM image [Figure 8B] of the reused catalyst showed no significant change from the initial state.

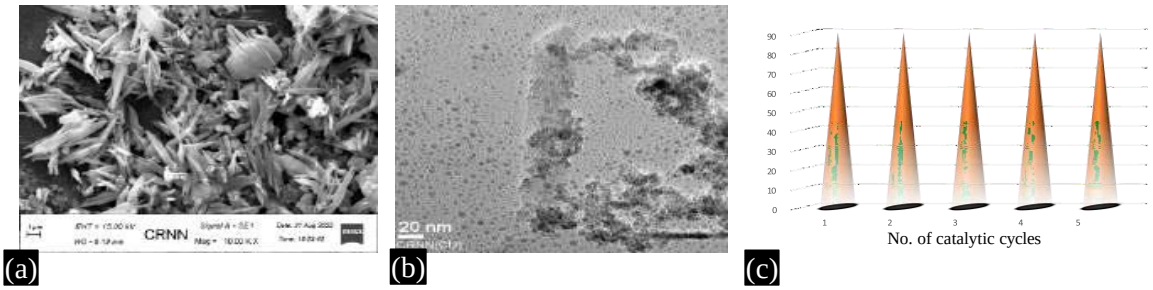

Figure 8. (a) SEM and (b) TEM Image of Reusable Catalyst After 5 Cycles of Nitroarenes Reduction and (c) Effect of the Reuse Catalyst Fe_3O_4@ISNA@NiL on Catalytic Efficiency for Nitroarenes Reduction.

CONCLUSION

In summary, we have successfully developed a heterogeneous catalyst, Fe_3O_4@ISNA@NiL, featuring a magnetic core. This catalyst exhibits remarkable efficiency in catalyzing the reduction of 4-nitrophenol (4-NP) to its corresponding aminophenol. Notably, the catalyst maintains its high level of activity over up to five consecutive reaction cycles without losing its catalytic activity, demonstrating its durability and reusability. The synthesis process employed is both straight forward and cost-effective making it practical for wide applications. Furthermore, the design approach utilized in this study has the potential to be extended for the development of other novel nanosystems with improved properties, potentially expanding their utility across a broad spectrum of advanced applications in various fields.

REFERENCES

1. Sahiner N, Yildiz S, LohedanHAl. The resourcefulness of p (4-VP) cryogels as template for in situ nanoparticle preparation of various metals and theiruseinH2production, nitrocompoundreductionanddye degradation. *Appl.Catal.B.*2015;166:145–54p.

2. Ibrahim I, Ali IO,Salama TM,et al.Synthesis of magnetically recyclable spinel ferrite (MFe_2O_4, M = Zn, Co, Mn) nanocrystals engineered by sol gel-hydrothermal technology: High catalytic performances for nitroarenes reduction. *Appl. Catal. B.*2016;181:389–02p.
3. Wu Z, Chen J, Di Q, et al.Size-controlled synthesis of a supported Ni nanoparticle catalyst for selective hydrogenation of p-nitrophenol to p-aminophenol. *Catal. Commun.* 2012;18:55–59p.
4. Zhou S, Wen M, Wang N, et al. Highly active NiCo alloy hexagonal nanoplates with crystal plane selective dehydrogenation and visible-light photocatalysis. *J. Mater. Chem.* 2012;22(33):16858–64p.
5. Ding J, Chen L, Shao R, et al. Catalytic hydrogenation of p-nitrophenol to produce p-aminophenol over a nickel catalyst supported on active carbon. *React. Kinet. Mech.Catal.* 2012;106(1):225–32p.
6. Abd El Maksod IH, Saleh TS. The use of nano supported nickel catalyst in reduction of p-nitrophenol using hydrazine as hydrogen donor. *Green Chem Lett. Rev.* 2010;3(2):127–34p.
7. Shen YY, Sun Y, Zhou LN, et al. Synthesis of ultrathin PtPdBi nanowire and its enhanced catalytic activity towards p-nitrophenol reduction. *J. Mater. Chem. A.* 2014;2(9):2977-84p.
8. Dasgupta S, Chatterjee S, Chattopadhyay T. Designing of a magnetically separable Fe_3O_4@ dopa@ ML nano-catalyst for multiple organic transformations (epoxidation, reduction, and coupling) in aqueous medium. *J. Coord. Chem.* 2019;*72*(3): 550–68p.
9. Poovan F, Chandrashekhar V G, Natte K, et al. Synergy between homogeneous and heterogeneous catalysis. *Catalysis Science & Technology*, 2022; *12*(22): 6623–49p.
10. Mondal R, Chakraborty A, Ghanta R, Menéndez M I, Chattopadhyay T. Experimental and theoretical investigation of the catalytic performance of reduced Schiff base and Schiff base iron complexes: Transformation to magnetically retrievable catalyst. *Appl. Organomet. Chem.* 2021; *35*(9): e6332p.
11. Xia J, He G, Zhang L, et al. Hydrogenation of nitrophenols catalyzed by carbon black-supported nickel nanoparticles under mild conditions. *Appl. Catal. B.* 2016;180:408–15p.
12. Zhang K, Suh JM, Choi JW, et al. Recent advances in the nanocatalyst-assisted $NaBH_4$ reduction of nitroaromatics in water. *ACS Omega.* 2019;4(1):483–95p.
13. Saha D. Potential of solid supported copper catalyst in sustainable organic synthesis. *RP Cur Tr Appl Sci.* 2024;3:10–13p.
14. Chakraborty T, Mondal R, Ghanta R, Chakraborty A, Chattopadhyay T. Triton X-100 functionalized Cu (II) dihydrazone based complex immobilized on Fe_3O_4@ dopa: A highly efficient catalyst for oxidation of alcohols, alkanes, and sulfides and epoxidation of alkenes. *Appl. Organomet. Chem.*2020;*34*(8): e5695p.
15. Singh P, Halder M, Ray S, et al. Biomolecule-mediated generation of Ru nanocatalyst for sustainable reduction of nitrobenzene. *ACS Omega.*2019;4(25):21267–78p.
16. Hasan K, Shehadi IA, Al-Bab ND, et al. Magnetic chitosan-supported silver nanoparticles: A heterogeneous catalyst for the reduction of 4-nitrophenol. *Catalysts.* 2019;9(10):839p.
17. Indra A, Greiner M, Gericke A K, Schlögl R, Avnir D, Driess M. High catalytic synergism between the components of the rhenium complex@ silver hybrid material in alkene epoxidations. *ChemCatChem*, 2014; *6*(7): 1935–39p.
18. Wang D, Li Y, Wen L, et al. Ni-Pd-incorporated Fe_3O_4 yolk-shelled nanospheres as efficient magnetically recyclable catalysts for reduction of N-containing unsaturated compounds. *Catalysts.* 2023;13(1):190p.
19. Thomas J M, Raja R. Designed open-structure heterogeneous catalysts for the synthesis of fine chemicals and pharmaceuticals. Stud. Surf. Sci. Catal. 2007; 170: 19–40p.
20. Frisch MJ, Trucks GW, Schlegel HB, et al. Gaussian 16, Revision A.03. *Wallingford, CT: Gaussian, Inc.*; 2016.
21. Becke AD. Density-functional thermochemistry. I. The effect of the exchange-only gradient correction. *J. Chem. Phys.* 1992;96(3):2155–60p.
22. Ghanta R, Mondal R, Chowdhury T, et al. Ni(II)-complex anchored over functionalized mesoporous SBA-15: A nanocatalyst for the synthesis of aminophenoxazinone derivatives. *ChemCatChem.* 2024;e202400653. doi: 10.1002/cctc.202400653.

23. Polshettiwar V, Baruwati B, Varma RS. Nanoparticle-supported and magnetically recoverable nickel catalyst: a robust and economic hydrogenation and transfer hydrogenation protocol. *Green Chem.* 2009;11(1):127–31p.
24. Mondal R, Chakraborty A, Zangrando E, et al. Synthesis of copper(II) complex-functionalized Fe_3O_4@ISNA (ISNA = isonicotinic acid) as a magnetically recoverable nanomaterial: catalytic studies in alcohol oxidation and nitrophenol reduction, and TD-DFT studies. *New J Chem.* 2024;48(16):7308–22p.
25. Zamani F, Kianpour S. Fast and efficient reduction of nitroaromatic compounds over Fe_3O_4/β-alanine-acrylamide-Ni nanocomposite as a new magnetic catalyst. *Catal. Commun.* 2014;45:1–6p.
26. Gowenlock CE, McGettrick JD, McNaughter PD, et al. Copper-complexed isonicotinic acid functionalized aluminum oxide nanoparticles. *Main Group Chem.* 2016;15(1):1–15p.
27. deAraújo EL, Barbosa HFG, Dockal ER, et al.Synthesis, characterization, and biological activity of Cu(II), Ni(II), and Zn(II) complexes of biopolymeric Schiff bases of salicylaldehydes and chitosan. *Int. J. Biol. Macromol.* 2017;95:168–76p.
28. Chakraborty A, Chowdhury T, Menéndez MI, et al. Iron complexes anchored onto magnetically separable graphene oxide sheets: an excellent catalyst for the synthesis of dihydroquinazoline-based compounds. *ACS Appl. Mater. Interfaces.*2020;12(34):38530–45p.
29. Adhikary J, Datta A, Dasgupta S, et al. Development of an efficient magnetically separable nanocatalyst: theoretical approach on the role of the ligand backbone on epoxidation capability. *RSC Adv.* 2015;5(112):92634–47p.
30. Verma CS, Shukla N, Bose P. Study of surface morphology and elemental investigation of chemically deposited mixed based photoconducting (Cdx-Pby-Znz)S films. *RP Mater Proc.* 2024;3(1):1–6p.
31. Singh N. Synthesis of SnO_2 nanoparticles by sol-gel method and their characterization. *RP Cur Tr Appl Sci.* 2023;2:30–33p.
32. Zhou W, Zhou Y, Liang Y, et al.Silver nanoparticles on carboxyl-functionalized Fe_3O_4 with high catalytic activity for 4-nitrophenol reduction. *RSC Adv.*2015;5(62):50505–11p.

